Identification of a Unique Transgenic Mouse Line That Develops Megabladder, Obstructive Uropathy, and Renal Dysfunction

Sunita Singh,* Melissa Robinson,* Fatin Nahi,* Brian Coley,† Michael L. Robinson,‡ Carlton M. Bates,* Karl Kornacker,§ and Kirk M. McHugh*

*Center for Cell and Developmental Biology, Columbus Children's Research Institute and †Department of Radiology, Columbus Children's Hospital, and §Division of Sensory Biophysics, The Ohio State University, Columbus, and ‡Zoology Department, Miami University, Oxford, Ohio

Urinary tract malformations, obstructive uropathy, and hypoplasia/dysplasia are extremely important in terms of pediatric health care costs, with end-stage renal failure in children estimated to cost >$15 billion annually in the United States alone. Even so, little is known regarding the mechanisms that control these processes. Identified was a unique mutant mouse model that develops *in utero* megabladder, resulting in variable hydroureteronephrosis and chronic renal failure secondary to obstructive uropathy. These animals, designated *mgb* for megabladder, possess a primary defect in bladder smooth muscle development that is apparent by embryonic day 15. The *mgb* mouse represents an excellent model for the study of normal and pathogenic bladder development, including the postnatal progression of chronic renal failure that results from the development of *in utero* obstructive uropathy.

J Am Soc Nephrol 18: 461–471, 2007. doi: 10.1681/ASN.2006040405

Fetal megabladder is a severe condition that has been shown to be associated with chromosomal abnormalities in 20 to 50% of the cases (1). Megabladder may present secondary to both partial and complete obstruction or to nonobstructive causes, including neurogenic and myopathic mechanisms (2,3). The most common cause of obstructive megabladder is posterior urethral valves, whereas myopathic megabladder is observed in megacystis-microcolon-intestinal hypoperistalsis syndrome, prune belly syndrome, and the development of bladder smooth muscle tumors. Congenital uropathies that cause *in utero* obstruction that leads to abnormal bladder development also have the potential to produce hydroureteronephrosis, renal impairment, and death. This direct link among bladder development, bladder function, and renal outcome represents a central paradigm of urogenital pathogenesis. That many of these changes are irreversible, especially when they occur *in utero*, may explain why a significant number of patients with outlet obstruction do not have complete recovery of bladder and/or kidney function after clinical intervention (4–6).

At this time, few functional models exist for the study of urogenital development and pathogenesis. In this study, we report the identification of a unique mutant mouse model that develops *in utero* megabladder that results in variable hydroureteronephrosis and renal insufficiency secondary to obstructive uropathy. Bladder smooth muscle defects are evident as early as embryonic day 15 in both genders of affected mice, with male mice exhibiting a more severe phenotype as development proceeds. These mice, designated *mgb* for megabladder, represent an excellent model for the study of normal and pathogenic bladder development and function, including the postnatal progression of chronic renal failure that results from *in utero* obstructive uropathy.

Received April 27, 2006. Accepted November 7, 2006.

Published online ahead of print. Publication date available at www.jasn.org.

Address correspondence to: Dr. Kirk M. McHugh, Columbus Children's Research Institute, 700 Children's Drive, Suite WA 2014, Columbus, OH 43205. Phone: 614-355-2817; Fax: 614-722-5892; E-mail: mchughk@ccri.net

Materials and Methods

Mice

FVB/N zygotes received a microinjection of a DNA construct that consisted of the coding sequences for the bovine sodium myoinositol co-transporter gene (*Slc5a3*) inserted between an αA- and αB-crystallin chimeric promoter (7) and SV40-derived intron and polyadenylation sequences from the lens crystallin vector CPV2 (8). DNA was injected and founder mice were identified as described previously (9,10). Mice were maintained according to the National Institutes of Health Guide for the Care and Use of Laboratory Animals. Initial characterization of the *mgb* mouse phenotype was performed by the Mouse Phenotyping Shared Resource (The Ohio State University), including survey radiographs, complete clinical chemistry, hematology characterization, and gross and microscopic examination of more than 40 tissues.

Morphology, Immunohistochemistry, and In Situ *Hybridization*

Embryos/tissues were isolated from mice with tail samples removed for genotyping. Specimens were processed in the Biomorphology Core using standard procedures (Columbus Children's Research Institute). The primary antibodies used in this study included α-smooth muscle isoactin diluted 1:100 (DakoCytomation, Carpinteria, CA), SMa22 di-

ISSN: 1046-6673/1802-0461

luted 1:20 (Novocastra Laboratories Ltd., Newcastle, UK), laminin diluted 1:30 (Sigma-Aldrich, St. Louis, MO), uroplakin diluted 1:50 (Fitzgerald Industries Int., Flanders, NJ), calponin diluted 1:500 (Sigma-Aldrich), and serum response factor (SRF) diluted 1:100 (Santa Cruz Biotechnology, Santa Cruz, CA). All antibodies were used according the conditions outlined by the suppliers. Detection of apoptotic cells was performed using the FragEL DNA Fragmentation Detection Kit as outlined by the supplier (Calbiochem, San Diego, CA). Radioactive *in situ* hybridization using ^{35}S-UTP radiolabeled riboprobes against Patched 1 receptor (*Ptc1*) (11) was performed on paraffin-embedded sections from embryonic day 13.5 (E13.5) and E15.5 mutant and control embryos as described previously (12). At least five or more mice of each genotype were examined for each antibody/stain/*in situ* discussed above.

Isolation of an MLR19-Positive BAC Clone

An MLR19 transgene-positive BAC clone, BAC5-4-E11-4, was isolated from an *mgb*−/− BAC genomic library that was commercially constructed using the pIndigoBAC-5 vector and screened by Bio S&T (Montreal, QU, Canada). Sequencing of the 100-kb BAC5-4-E11-4 insert was performed by the Sequencing Core Facility (Columbus Children's Research Institute) using standard techniques. Sequence was read using ABI Prism 31 30×1Genetic Analyzer (Applied Biosystems, Foster City, CA), and analysis was done through BLAST and MacVector 8.0.2 (Accelrys Software, San Diego, CA).

Fluorescence In Situ *Hybridization Analysis*

Fluorescence *in situ* hybridization analysis was performed with an MLR19 transgene-positive BAC clone using standard techniques in the Molecular Cytogenetics Core at The Ohio State University. Briefly, bone marrow was aspirated from the femur of transgenic and wild-type mice and grown overnight in RPMI medium supplemented with 15% FBS. Cells were harvested using standard cytogenetics methods and stored in Carnoy's fixative at −20°C. BAC DNA for fluorescence *in situ* hybridization analysis was isolated using the Spin Doctor BAC Prep kit according to the conditions outlined by the supplier (Gerard Biotech, Oxford, OH). BAC probes were labeled with Spectrum Orange, Spectrum Green, or Spectrum Aqua using a nick translation kit according to the manufacturer's recommendations (Vysis, Downer Groves, IL). BAC DNA was combined with mouse Cot-1 DNA, ethanol precipitated, resuspended in hybridization buffer (Sigma), and denatured. Probes were applied to fresh denatured slides, and hybridization was carried out overnight at 37°C. Slides were washed in 2× SSC/0.1% NP-40 for 5 min at 42°C. Fluorescence signals were viewed with a Zeiss Axioscope 40 microscope and analyzed with the Applied Imaging System (Zeiss, Thornwood, NY). For G-banding pattern, the fixed cell suspension was dropped onto precleaned, warm, wet slides. The slides were aged at 90°C for 1 h, banded with trypsin, and stained with Wright's stain. Banded metaphase chromosomes were analyzed as described previously.

PCR and Genotyping

DNA was isolated using the Spin Doctor Genomic DNA Isolation kit according to the manufacturer's protocol (Gerard Biotech). Primers 5′-GCATTCCAGCTGCTGACGGT-3′ and 5′-CGCCCCGCCAAGAAGTATCCA-3′ were used to identify *mgb* transgene-positive mice *via* amplification of a 487-bp band at 95°C for 5 min (95°C for 30 s, 57°C for 30 s, and 72°C 60 s) × 30 and 72°C for 10 min. Gender was identified using primers 5′-TGAAGCTTTTGGCTTTGAG-3′ and 5′-CCGCTGCCAAATTCTTTGG-3′ as described previously (13). PCR product was confirmed by DNA gel electrophoresis.

Real-time PCR genotyping was performed using primers 5′-CAACCGACTCTGCATTCATCTC-3′ and 5′-CTCCAGTACAGCCCTCATGTTTG-3′ specific for the *mgb* MRL19 transgene with the probe 6FAMAAGCTTGATATCGAATTCMGBNFQ. Glucagon was used as an internal control with primers 5′-CACAACATCTCGTGCCAGTCA-3′ and 5′-ATCTGCATGCAAAGCAATATAGCT-3′ using the probe VICTGGGATGTACAATTTCAAMGBNFQ. Concentration for primers and probes were 18 and 5 μM, respectively. Reactions were performed in triplicate with 20 ng of DNA and TaqMan Universal PCR Master Mix, No AmpErase UNG using the ABI Series 7500 (Applied Biosystems). Reaction conditions were 95°C for 10 min (95°C for 15 s, 60°C for 60 s) × 40. Data were analyzed using ABI 7500 System Sequence Detection Software Version 1.2.3 (Applied Biosystems).

Fluid Studies and Cystometry

Urine output and water intake were monitored for 24 h using the Metabolic Cage System for Rodents (Harvard Biolabs, Cambridge, MA). For cystometry, mice were sedated using inhaled isoflurane, and ultrasound imaging was performed with a broadband high-frequency linear transducer (12 to 5 MHz) using a Philips HDI 5000 optimized for small parts imaging (Philips, Bothell, WA). Bladders were aspirated under ultrasound guidance to determine urine volume. Iodinated contrast media (Optiray 240; Ioversol Mallinckrodt, St. Louis, MO) was instilled by gravity from a height of 30 cm. Filling was monitored by intermittent fluoroscopy and halted when spontaneous voiding occurred.

Statistical Analyses

Mice were anesthetized with inhaled isoflurane, and 100 to 200 μl of blood was collected from the periorbital sinus. Serum was separated by centrifugation at 8000 rpm for 10 min at 23°C and analyzed by the Mouse Phenotyping Core (The Ohio State University) for renal panel and blood chemistry using a Hitachi 911 Automatic Analyzer (Boehringer Mannheim, Indianapolis, IN). Serum electrolyte levels were determined using a Nova 8 CRT. Individual blood test results were compared with the median of the corresponding same-gender wild-type results, and the magnitude of the log2 ratio was used to measure the individual degree of abnormality. An exact upper-tailed Wilcoxon rank-sum test was used to determine whether the abnormality measures were elevated significantly relative to the corresponding same-gender wild-type mice. Individual blood chemistry values were considered significant when the NLP value exceeded 2.3 or $P = 0.005$.

Results

Identification of a Unique Mutant Mouse Model

We have identified a unique transgene-induced mutation in the mouse line *MLR19* that develops *in utero* megabladder that results in variable hydroureteronephrosis (Figure 1). The *MLR19* transgene is a bovine sodium myoinositol co-transporter gene that is driven by a chimeric αA-crystallin/αB-crystallin promoter that is designed to direct transgene expression in the lens. During production of these mice, the *MLR19* transgene randomly inserted into mouse chromosome 16 between 26.6 and 27.5 Mb (Table 1). The transgene in conjunction with a portion of chromosome 16 then translocated into a second domain on chromosome 11, resulting in the development of megabladder in homozygotic mice (Figure 2). Two other independent transgenic lines that were made with the identical transgene construct, as well as several other transgenic lines that overexpress the same genes, did not exhibit the

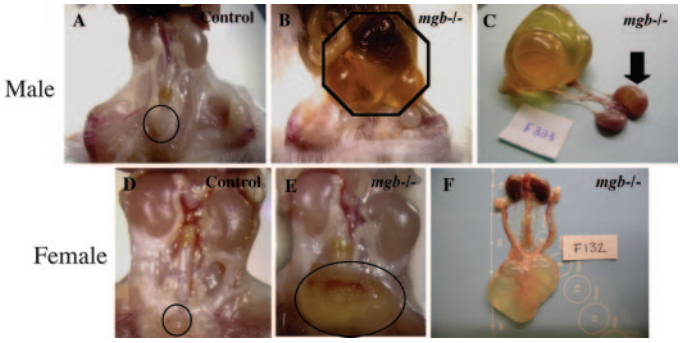

Figure 1. Homozygotic *mgb* mice develop megabladder and hydronephrosis. Postnatal day 17 control male mouse bladder (A, circle) *versus* male *mgb*−/− mouse shows severely enlarged bladder (B, hexagon, and C) and grossly evident hydronephrotic kidney (C, arrow). Postnatal day 12 control female mouse bladder (D, circle) *versus* female *mgb*−/− mouse shows enlarged bladder (E, oval, and F).

Table 1. Sequence and chromosome identification of the MLR19 transgene-positive BAC clone[a]

BAC Clone Number	Chromosome ID	Sequence ID
3S	16	26670910–26671243
3N	16	26671505–26671805
19N	16	26673843–26674197
14N	16	26678126–26678519
17N	16	26679089–26679481
7N	16	26681817–26681994
7S	16	26682343–26682560
4S	16	26684148–26684424
18N	16	26684523–26684912
1S	16	26699608–26699723
1N	16	26700242–26700356
5S	16	26707829–26707989
9N	16	26720601–26720686
9S	16	26721230–26721317
2N	16	27501149–27501450
2S	16	27501730–27501878

[a]Sequence identification is reported as base pairs referencing the Ensembl Database (www.ensembl.org).

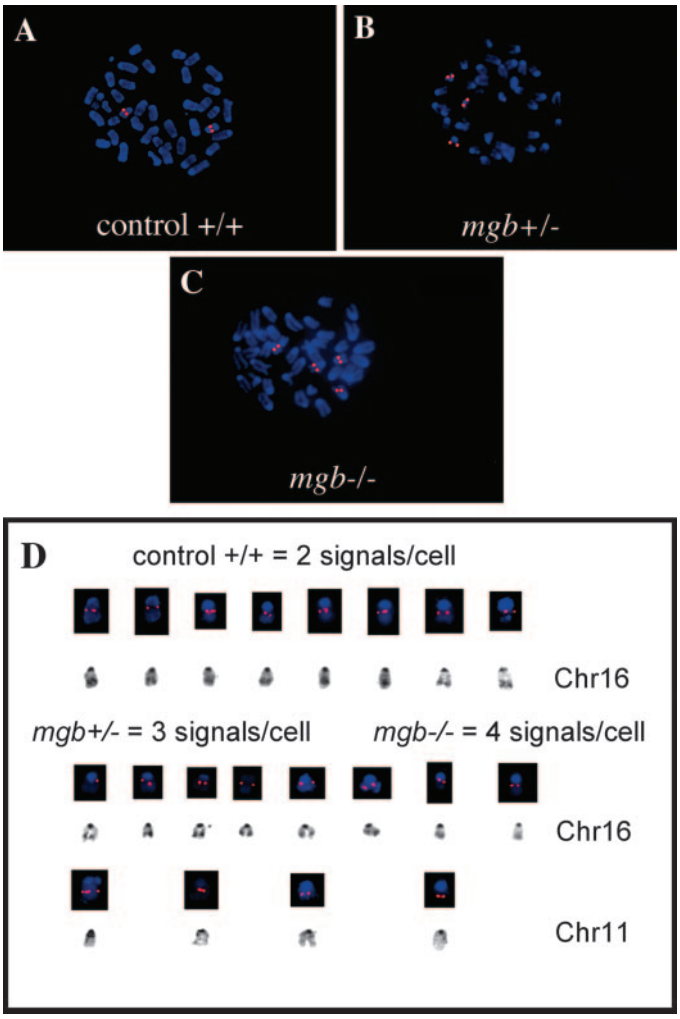

Figure 2. Homozygotic *mgb* mice show transgene insertion into a region of chromosome 16 that then is translocated to chromosome 11. Representative fluorescence *in situ* hybridization (FISH) (A through C) and karyotype analysis (D) of control (A), *mgb*+/− (B), and *mgb*−/− (C) chromosome spreads probed with an MLR19 BAC clone that contains the transgene and a subfragment of chromosome 16. Note the two paired FISH signals in control mice, indicating the presence of two normal copies of chromosome 16 (A). In contrast, *mgb*+/− (B) and *mgb*−/− (C) mice contain three and four signals, respectively, indicating the translocation of the transgene that contains a subfragment of 16 to a second chromosome, which was identified by karyotype analysis as chromosome 11 (D).

mgb phenotype. Breeding with *C57BL/6* mice produced an identical phenotype in the F2 generation, indicating that the *mgb* phenotype does not depend strictly on the *FVB/N* genetic background.

At birth, homozygous megabladder (*mgb*−/−) male mice show obvious signs of severe bladder distension, exhibit a rapid pathologic progression, and rarely survive beyond 4 to 6 wk of age. In comparison, *mgb*−/− female mice show a much slower pathologic progression, developing overt megabladder much later in life. At E15, when the bladder phenotype first becomes evident, all other organ systems, including the kidneys, appear normal (Supplemental Figure 1). Adult heterozygotic megabladder (*mgb*+/−) mice seem phenotypically normal. During the examination of 144 *mgb* offspring that resulted from interbreeding of two *mgb*+/− mice, we identified 32 wild-type +/+, 79 *mgb*+/−, and 33 *mgb*−/− (17 male and 16 female) using real-time PCR to determine transgene copy number (Table 2). These results indicate that the *mgb* phenotype is an autosomal recessive mutation with no gender bias.

mgb Mice Develop Megabladder and Hydroureteronephrosis

Analysis of adult *mgb*−/− mice revealed profound changes in bladder morphology, including severe distention and a dra-

Table 2. Representative real-time PCR genotyping data showing MLR19 transgene copy number[a]

Genotype	Transgene Copy Number
Wild-type+/+	0.00
Wild-type+/+	0.00
Wild-type+/+	0.01
mgb+/−	1.00
mgb+/−	1.00
mgb+/−	1.08
mgb+/−	1.10
mgb−/−	1.82
mgb−/−	1.99
mgb−/−	2.14
mgb−/−	2.28
mgb−/−	2.45

[a]Transgene copy number is represented as the relative quantification (RQ) PCR value and was used to genotype mice with wild-type mice that possessed zero copies of the MLR19 transgene, *mgb*+/− mice that possessed one copy of the MLR19 transgene, and *mgb*−/− mice that possessed two copies of the MLR19 transgene. All values represent an average of at least three independent experiments and were normalized to an internal glucagon control and calibrated to *mgb*+/− = 1.0.

matic thinning of the bladder wall (Figure 3, A and B). The most striking histologic feature of the *mgb*−/− megabladder was its nearly complete lack of muscularis, whereas the lamina propria showed modest signs of regional disorganization and hypervascularization. Although occasional small regions of multilayered smooth muscle were observed, the majority of the bladder wall possessed no detectable smooth muscle. The *mgb*−/− mice routinely developed hydroureteronephrosis with severely distended ureters and kidneys that possessed a grossly distended renal pelvis and highly compressed parenchyma (Figure 3, C through F).

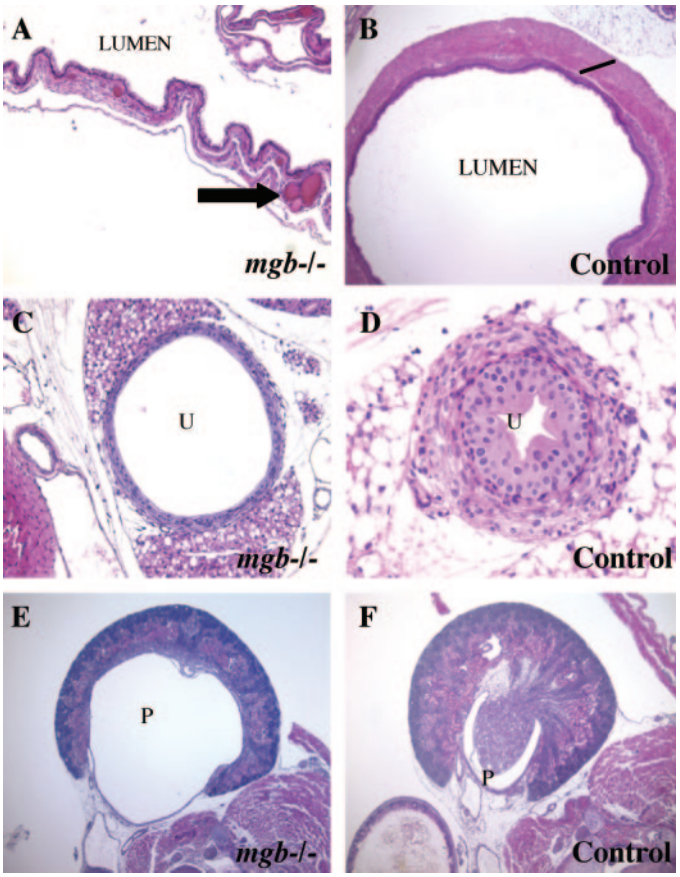

Figure 3. Homozygotic *mgb* bladders lack a defined smooth muscle layer, and homozygotic *mgb* mice develop hydroureteronephrosis. Representative hematoxylin and eosin staining of bladders in postnatal day 22 *mgb*−/− (A) and control (B) mice, ureters (U) in postnatal day 22 *mgb*−/− (C) and control (D) mice, and kidneys in postnatal day 1 *mgb*−/− (E) and control (F) mice. Note the complete lack of muscularis in the *mgb*−/− megabladder (A) when compared with control (B, bar) and the development of severe hydroureter (C) and hydronephrosis (E) including dilation of the renal pelvis (P) in *mgb*−/− mice. Arrow in A indicates region of hypervascularization in the lamina propria of *mgb*−/− bladders. Magnifications: ×100 in A and B; ×200 in C; ×400 in D; ×50 in E and F.

mgb−/− *Mice Develop* In Utero *Megabladder*

Analysis of E18 *mgb*−/− mice revealed the clear development of overt *in utero* megabladder in a subset of male and female mice (Figure 4, A through C). In affected *mgb*−/− embryos, a gender-based difference in the progression of megabladder seemed apparent. Male E18 megabladders possessed a morphology similar to that observed in adult *mgb*−/− mice, in which the bladder was severely distended and thin walled and lacked any significant smooth muscle layer. In contrast, female E18 megabladders seemed to display a less severe morphologic phenotype, with a moderately distended bladder that possessed a thin but continuous ring of smooth muscle.

mgb−/− *Mice Have Altered Bladder Smooth Muscle Development*

Uroplakin staining indicated that urothelial development seemed normal in E15 *mgb*−/− mice (Supplemental Figure 2). Even so, the luminal opening of *mgb*−/− bladders often appeared smaller than either control or *mgb*+/− bladders. This condition may reflect simply a sectioning artifact, as more "open" *mgb*−/− lumens are routinely observed. However, it also is plausible that luminal patency depends partially on the tensile strength that is generated by the developing detrusor smooth muscle, resulting in partial contraction of the urothelium and reduction of the luminal opening in the amuscular *mgb*−/− bladders.

We examined the initiation of smooth muscle development in E15 *mgb*−/− mice using α-smooth muscle isoactin expression as a marker of smooth muscle myoblast differentiation (Figure 4, D through P). The *mgb*−/− bladders showed a lack of condensation of the peripheral mesenchyme, resulting in clusters of differentiating smooth muscle myoblasts separated by regions of undifferentiated mesenchyme, producing a highly disorganized presumptive muscle layer (Figure 4, G through I).

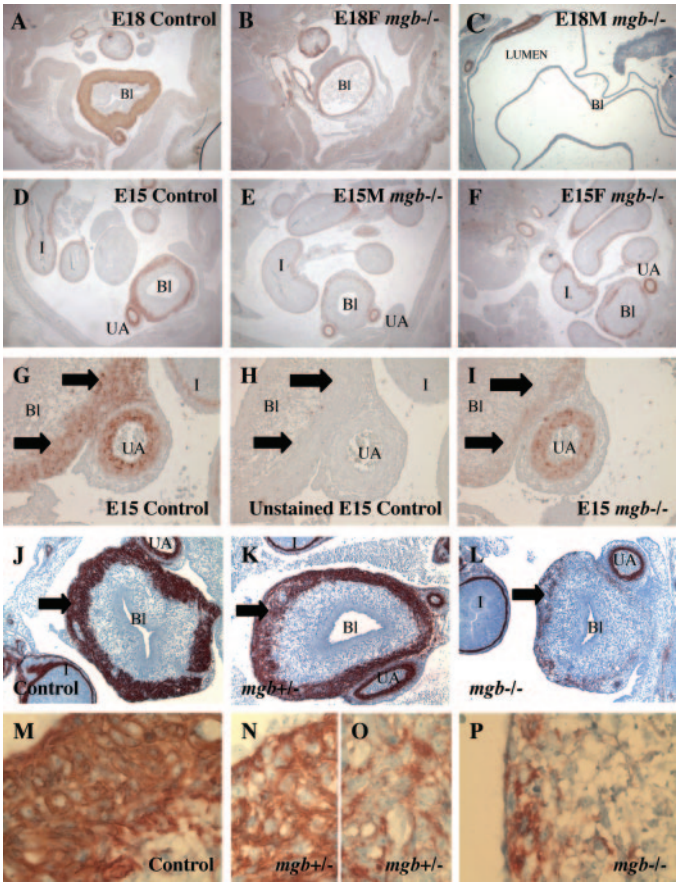

Figure 4. Homozygotic *mgb* mice develop *in utero* megabladder by embryonic day 18 (E18), resulting from a defect in bladder smooth muscle development. Representative α-smooth muscle isoactin expression indicated by brown immunohistochemical staining in E15 and E18 male (M) and female (F) control (A, D, G, H, J, and M), *mgb*+/− (K, N, and O), and *mgb*−/− (B, C, E, F, I, L, and P) bladders (Bl), umbilical artery (UA), and intestine (I). AT E15 (D through F), incomplete smooth muscle differentiation is observed in *mgb*−/− bladders (E and F) *versus* control (D), whereas equivalent normal staining of α-smooth muscle isoactin is apparent in the developing intestine (I) and umbilical artery (UA) of all three mice. Note the clearly demarcated ring of condensing mesenchyme in control bladder (H, arrows) that shows robust α-smooth muscle isoactin staining in these cells (G, arrows) *versus* the lack of condensing mesenchyme in the *mgb*−/− bladder that showed diffuse, poorly organized α-smooth muscle isoactin staining (I, arrows). The umbilical artery in the same section shows normal α-smooth muscle isoactin staining when compared with the control (I *versus* G). The variability in thickness and density of α-smooth muscle isoactin staining in each genotype (J through L, arrows) suggests the presence of an intermediate phenotype in *mgb*+/− mice. The intermediate *mgb*+/− muscle phenotype is obvious showing regions similar in appearance to control (N *versus* M) as well as *mgb*−/− (O *versus* P) developing smooth muscle layers. Magnifications: ×50 in A through F; ×400 in G through I; ×200 in J through L; ×1000 in M through P.

No difference in the defect was observed between E15 male and female *mgb*−/− mice. It is interesting that E15 *mgb*+/− bladders displayed an intermediate smooth muscle phenotype with normal regions of mesenchymal compaction interspersed between slightly less compacted regions that seemed very similar to the *mgb*−/− bladder (Figure 4, J through P). Identical muscle defects were observed using additional markers of smooth muscle development, including calponin (Figure 5) and SMα22 (Supplemental Figure 3). Remarkably, smooth muscle differentiation seemed normal in the developing gastrointestinal, vascular, and respiratory tracts of *mgb*−/− mice, suggesting that the smooth muscle defect that is associated with *mgb* phenotype is bladder specific.

SRF, a key transcription factor that regulates smooth muscle development, including the expression of α-smooth muscle isoactin, calponin, and SMα22, showed robust nuclear staining within smooth muscle cells of control bladders (Figure 5). In contrast, the presumptive smooth muscle layer of the *mgb*−/− bladder possessed almost undetectable levels of SRF expression (Figure 5, K and L), whereas *mgb*+/− bladders showed mixed, intermediate levels of SRF expression (Figure 5, G and H). This observation suggests that the defect in *mgb*−/− bladders is upstream of the SRF signaling pathway.

In an effort to determine whether the *mgb*−/− bladder lacked proper development of the mesenchymal precursors that are necessary for the formation of bladder smooth muscle, we examined patched expression in E13 and E15 bladders (Figure 6). The density of mesenchymal cells and the intensity of patched expression within the peripheral mesenchyme of the presumptive E13 *mgb*−/− bladder seemed normal when compared with control. In addition, the spatial shifting of patched expression from the peripheral mesenchyme to the underlying submucosal region of the developing urothelium was present at E15 in both normal and *mgb*−/− bladders. This analysis indicates that patched expression is regulated normally during *mgb*−/− bladder development, suggesting that the defect in *mgb* mice lies downstream of this signaling pathway.

Terminal deoxynucleotidyl transferase–mediated dUTP nick-end labeling analysis indicated that no significant apoptotic signal was observed in E13, E18, and newborn control and *mgb*−/− bladders (Figure 7). In contrast, a five- to 10-fold increase in apoptosis was observed in E15 *mgb*−/− bladders *versus* control (Figure 7, C and D). It is interesting that >90% of the apoptotic cells that were detected in E15 *mgb*−/− bladders were restricted to the presumptive muscle layer within the peripheral half of the developing mesenchyme. This observation provides a mechanism for the selective elimination of developing smooth muscle cells in *mgb*−/− bladders, potentially explaining their absence in the adult.

Urine Output in mgb−/− *Mice*

In general, no significant differences in mean water intake and mean urine output were observed between *mgb* genotypes; however, two exceptions were noted (Figure 8A). First, one female *mgb*+/− mouse displayed polydipsia and polyuria, drinking more than three times as much water and producing more than 10 times as much urine as her genetic counterparts. Second, none of the age-matched *mgb*−/− weanlings examined produced any measurable urine output as detected by the metabolic cage. Because of the severity of their condition, only

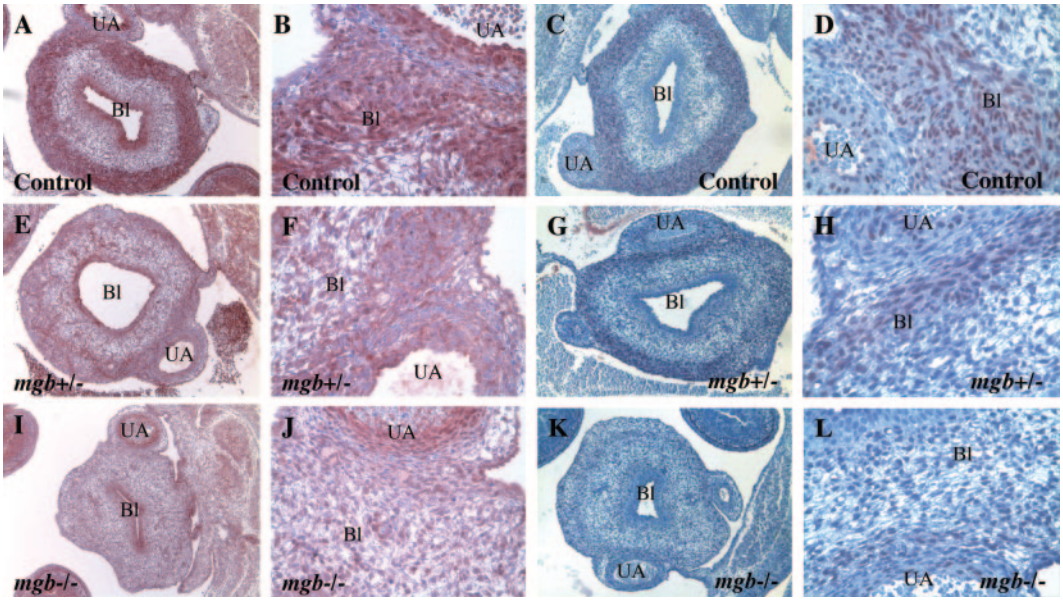

Figure 5. Both homozygotic and heterozygotic *mgb* bladders show alterations in calponin and serum response factor (SRF) expression. Representative calponin (A, B, E, F, I, and J) and serum response factor (C, D, G, H, K, and L) expression indicated by brown immunohistochemical staining in E15 control (A through D), *mgb*+/− (E through H), and *mgb*−/− (I through L) bladders (Bl) and umbilical artery (UA) at low (A, C, E, G, I, K) and high (B, D, F, H, J, L) power. Note lack of calponin and SRF expression in *mgb*−/− presumptive muscularis (I through L) and intermediate levels of expression in *mgb*+/− muscularis (E through H) when compared with controls (A through D). Magnifications: ×50 in A, C, E, G, I, and K; ×200 in B, D, F, H, J, and L.

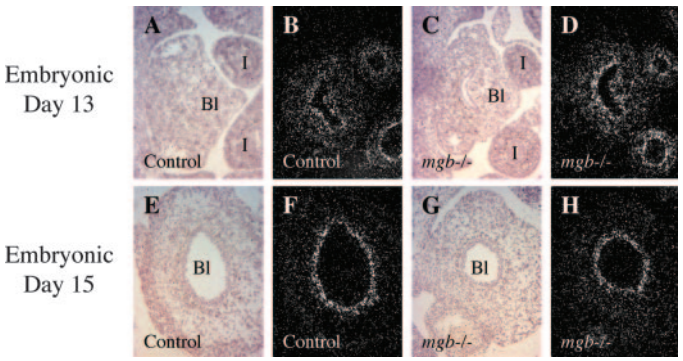

Figure 6. Homozygotic *mgb* mice show normal mesenchymal patterning at E15. Representative bright-field (A, C, E, and G) and dark-field (B, D, F, and H) *in situ* analysis of patched 1 receptor expression in E13 (A through D) and E15 (E through H) control and *mgb*−/− bladders (Bl) and intestine (I). Note identical patterns of patched 1 expression between control and *mgb*−/− mice at both E13 and E15.

one male *mgb*−/− weanling survived the 24-h testing period. In an effort to characterize further the potential urine output of these mice, we performed percutaneous drainage of male *mgb*−/− bladders, removing an average of 10 to 15 ml of urine. Within 1 to 2 h of drainage, male *mgb*−/− bladders completely refilled with urine, suggesting the presence of severe concentration defects in these mice.

Because the male *mgb*−/− mice that were examined in the metabolic study expressed no detectable urine, we performed cystometry on live mice in an effort to determine whether the urethra was occluded. Consistent with our morphologic studies, baseline cystograms showed grossly enlarged, trilobular bladders in *mgb*−/− mice *versus* normal controls (Supplemental Figure 4). When contrast reagent was reservoir fed into the male *mgb*−/− bladder, it resulted in the extrusion of liquid through the urethra, suggesting that the male urethra is patent when sufficient fluid backpressure is generated within the *mgb*−/− bladder.

mgb−/− Mice Develop Altered Serum Chemistry

In an effort to determine the degree of renal insult associated with the *mgb* phenotype, we performed blood chemistry profiles on 30 *mgb*−/−, 17 *mgb*+/−, and 12 wild-type female mice and 30 *mgb*−/−, 23 *mgb*+/−, and 16 wild-type male mice (Figure 8, B through E). Nine key blood chemistry parameters were examined for each mouse, including blood urea nitrogen (BUN), creatinine, phosphorus, calcium, sodium, potassium, chloride, bicarbonate, and albumin. No statistically significant alterations in serum blood chemistry were observed between wild-type and female *mgb*+/− and *mgb*−/− mice. In contrast, statistically significant increases in BUN, creatinine, calcium, and potassium were observed in male *mgb*−/− mice when compared with controls. It is interesting that male *mgb*+/− mice also showed a statistically significant increase in potassium as well as chloride even though they seemed phenotypically normal.

Because the development of renal insult in *mgb*−/− mice is variable over time, the serum chemistry values displayed a wide range of variance, depending on the precise disease state of the mouse examined. At any given time point, individual

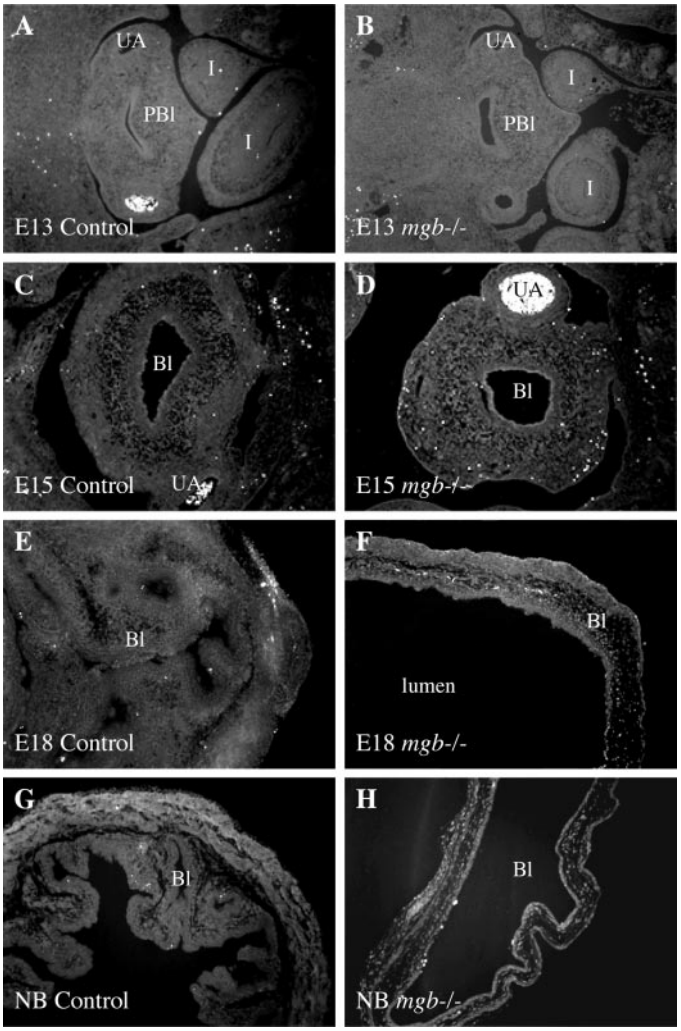

Figure 7. Homozygotic *mgb* bladders show an increase in cell death within the mesenchymal compartment at E15. Representative terminal deoxynucleotidyl transferase–mediated dUTP nick-end labeling staining indicated by white dots in E13, E15, E18, and newborn (NB) control (A, C, E, and G), and *mgb*−/− (B, D, F, and H) presumptive bladders (PBl), bladder (Bl), umbilical artery (UA), and intestine (I). Note lack of significant apoptotic signal in E13, E18, and NB control (A, E, and G) and *mgb*−/− bladders (B, F, and H) compared with an increase in apoptotic signal in the peripheral half of E15 *mgb*−/− mesenchyme (D) *versus* control (C).

mgb−/− mice may show highly significant differences in serum chemistry values when compared with controls. However, when these values were averaged over multiple mice, their statistical significance was lost. Even so, we were able to identify a subset of eight male and four female *mgb*−/− mice that all displayed bicarbonate levels <5.0 and routinely had dramatically increased BUN and creatinine levels (Tables 3 and 4). Parenthetically, these same mice often were noted as terminally sick mice that had to be killed within 24 to 48 h of serum sampling. Of the *mgb*−/− mice identified in this pool, eight had grossly evident signs of severe hydronephrosis, whereas the other four were not recorded. It is interesting that in a statistical analysis of all nine blood chemistry parameters examined for an individual mouse, a sum of the observed changes in BUN, creatinine, and bicarbonate generated a "disease state" marker that successfully identified these 12 *mgb*−/− mice as the most severely effected mice within this study.

Discussion

In this study, we identified a unique mutant mouse model that develops *in utero* megabladder. Histologic analysis revealed profound changes in bladder morphology, the most striking feature of which was a lack of detrusor smooth muscle in the adult bladder. Previous studies indicated that bladder smooth muscle differentiates in the peripheral half of the mesenchyme at approximately E15 in the mouse and is marked initially by mesenchymal compaction followed by the appearance of α-smooth muscle actin–positive myoblasts within the condensing mesenchyme (14). Short-axis patterning in the bladder smooth as well as other smooth muscle tissues is controlled by reciprocal epithelial-mesenchymal induction that involves the expression of the hedgehog family of proteins, patched receptor, Gli family of proteins, and bone morphogenic protein family of proteins (11,15–21). The later progression of smooth muscle myoblasts to fully differentiated myocytes is mediated by the cooperative expression of SRF and myocardin within the developing smooth muscle cells (22–25).

The lack of overt mesenchymal compaction in *mgb*−/− bladders suggests that the defect in these mice involves the early stages of short-axis patterning of the developing bladder. However, analysis of patched 1 receptor expression indicated normal patterning of *mgb*−/− bladder mesenchyme during the initial stages of smooth muscle development. Because patched expression is regulated directly by sonic hedgehog expression (11), these results suggest that this critical signaling pathway is functional in *mgb*−/− bladders. Even so, the developmental complexity of short-axis patterning would provide many additional targets for disruption in the *mgb*−/− mouse, and studies are under way to investigate these additional signaling pathways.

The expression of three distinct markers of smooth muscle differentiation was disrupted in *mgb*−/− bladders, as was the expression of SRF, a key transcription factor that regulates the expression of each of these genes. This disruption in the developmental progression from smooth muscle myoblast to smooth muscle myocyte was tissue specific, indicating that this developmental program was altered selectively in *mgb*−/− bladders. The presence of small clusters of differentiating smooth muscle myoblasts within *mgb*−/− bladders suggests that smooth muscle differentiation was capable of initiating in these mice, further supporting the observation that short-axis patterning is at least partially functional in these mice.

Previous studies indicated that the progression of smooth muscle development from myoblast to myocyte requires the close association of differentiating smooth muscle cells (26,27). Because *mgb*−/− bladders seem to initiate smooth muscle myoblast formation in the absence of mesenchymal compaction, it seems plausible that smooth muscle development within the *mgb*−/− bladder is abrogated at the myoblast stage. This hy-

pothesis is supported by a selective increase in apoptosis within the muscular compartment of developing E15 *mgb*−/− bladders, which suggests that smooth muscle myoblasts may be undergoing cell death before overt smooth muscle myocyte differentiation can occur, resulting in their selective loss from the *mgb*−/− bladder.

The bladder specificity of the *mgb*−/− defect is remarkable when one considers that smooth muscle differentiation in the developing gastrointestinal tract, respiratory tract, and vasculature system of these mice seems perfectly normal. Previous studies showed that the pattern of smooth muscle differentiation in the developing bladder is distinct from that observed in other developing smooth muscle tissues, suggesting that the inductive signals that are responsible for detrusor smooth muscle differentiation may be unique (14). This observation provides a potential mechanistic platform for the bladder specificity of the defects that are observed in *mgb*−/− mice.

The poor initiation of smooth muscle development within the *mgb*−/− bladder leads to the formation of a nonfunctional, amuscular bladder in the adult. This congenital defect in bladder smooth muscle development produces the functional equivalent of a lower urinary tract obstruction in *mgb*−/− mice, which results in the development of variable hydroureteronephrosis and renal insufficiency secondary to this condition. The severity of this condition is variable between mice, with a subset of mice developing *in utero* megabladder and hydroureteronephrosis as early as E18. Male *mgb*−/− mice consistently show a faster progression and more severe presentation than female *mgb*−/− mice. Serum chemistry data support this observation indicating that male *mgb*−/− mice possess increases

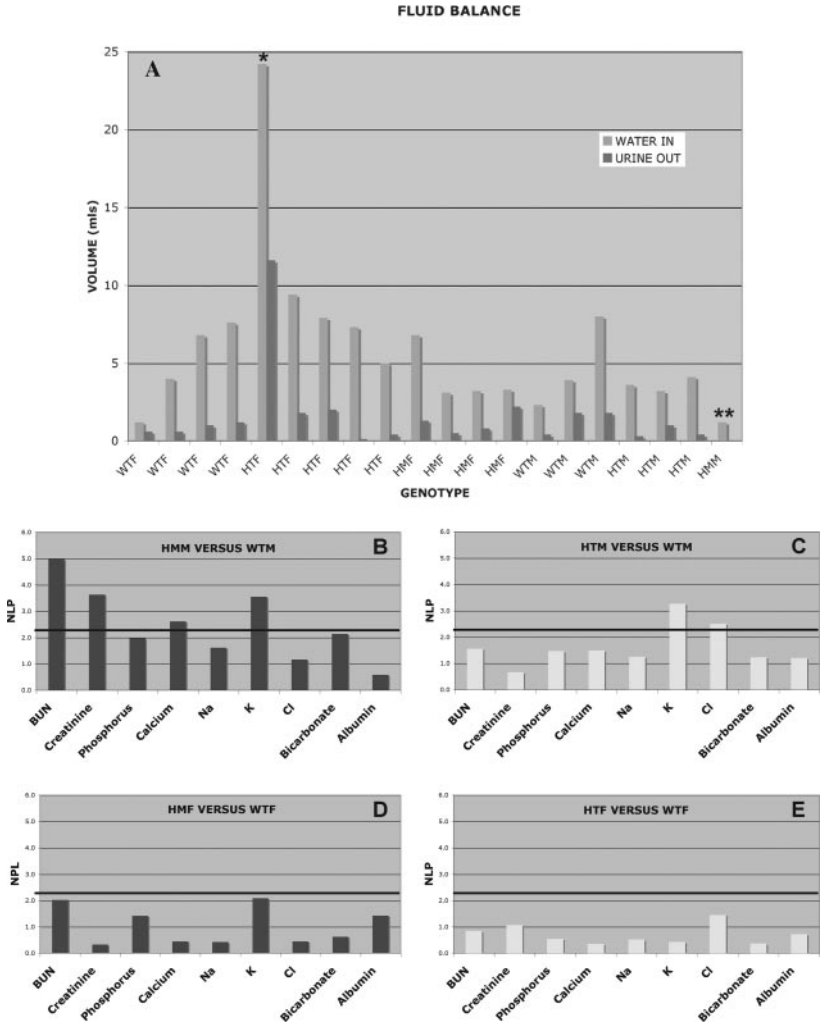

Figure 8. Homozygotic *mgb* mice show alterations in fluid balance and serum chemistry. Fluid balance (A) in wild-type female (WTF), *mgb*+/− female (HTF), *mgb*−/− female (HMF), wild-type male (WTM), *mgb*+/− male (HTM), and *mgb*−/− male (HMM) how water intake (light gray) *versus* urine output (dark gray) during a 24-h collection period. A large degree of variability was observed within genotypes with no statistically significant differences observed between phenotypes. Two exceptions were noted, including one female *mgb*+/− mouse (*) that displayed polydipsia and polyuria and one *mgb*−/− male mouse (**) that survived the 24-h testing period with no detectable urine output. Statistical analysis of serum chemistry values for HMM (B), HTM (C), HMF (D), and HTF (E) *versus* WT.

Table 3. Blood chemistry and kidney morphology in male *mgb−/−* mice[a]

Genotype	Hydronephrosis	BUN	Creatinine	P	Ca	Na	K	Cl	Bicarbonate	Albumin
0 to 2 HMM	+++	**153**	**2.7**	**32.7**	**10.2**	129	**18.3**	*87*	*<5.0*	*0.21*
0 to 2 HMM	+++	**40**	0.4	**12.0**	9.2	132	5.6	84	*<5.0*	2.0
0 to 2 HMM	+++	*20*	—	**13.2**	**9.6**	**136**	**6.0**	**88**	*<5.0*	**3.2**
3 to 4 HMM	+++	**740**	**11.0**	**94.1**	9.3	*87*	**80.3**	83	*<5.0*	*0.8*
3 to 4 HMM	+++	**99**	0.3	**15.0**	10.5	**159**	**8.1**	**108**	*<5.0*	**3.3**
3 to 4 HMM	+++	**27**	0.3	**13.2**	—	**150**	—	90	*<5.0*	**3.3**
3 to 4 HMM	ND	**84**	**0.6**	**13.8**	9.6	144	**9.6**	**108**	*<5.0*	—
5+ HMM	ND	**84**	**0.6**	**13.8**	**9.6**	144	**9.6**	**108**	*<5.0*	**4.2**

[a]Blood chemistry values were correlated with gross kidney morphology for terminally ill mice that demonstrated a decrease in bicarbonate of <5.0 and/or dramatic increases in blood urea nitrogen (BUN) and creatinine. Genotypes recorded included 0- to 2-wk-old, 3- to 4-wk-old, and 5+-wk-old *mgb−/−* male (HMM) mice. Blood chemistry values are shown as statistically increased (bold) or decreased (italic) from normal (plain). Hydronephrosis was graded as slight (+), moderate (++), or severe (+++). ND, not done; — error value recorded. A summation of the changes observed in BUN, creatinine, and bicarbonate provided the best prognostic marker of terminally ill mice.

Table 4. Blood chemistry and kidney morphology in female *mgb−/−* mice[a]

Genotype	Hydronephrosis	BUN	Creatinine	P	Ca	Na	K	Cl	Bicarbonate	Albumin
0 to 2 HMF	+++	**220**	0.3	16.0	10.8	**152**	**6.8**	100	*<5.0*	2.8
5+ HMF	+++	**366**	**3.2**	**30.2**	**12.2**	142	**8.8**	*92*	7.2	**3.6**
5+ HMF	ND	**164**	**1.4**	**11.8**	—	**154**	—	106	*<5.0*	2.8
5+ HMF	ND	**218**	**1.8**	**23.6**	**10.9**	141	**37.8**	**114**	10.0	—

[a]Blood chemistry values were correlated with gross kidney morphology for terminally ill mice that demonstrated a decrease in bicarbonate of <5.0 and/or dramatic increases in BUN and creatinine. Genotypes recorded included 0- to 2-wk-old, 3- to 4-wk-old, and 5+-wk-old *mgb−/−* female (HMF) mice. Blood chemistry values are shown as statistically increased (bold) or decreased (italic) from normal (plain). Hydronephrosis was graded as slight (+), moderate (++), or severe (+++). A summation of the changes observed in BUN, creatinine, and bicarbonate provided the best prognostic marker of terminally ill mice.

in BUN and creatinine levels that are consistent with the rapid development of renal insufficiency, whereas female *mgb−/−* mice do not. Even so, individual female *mgb−/−* mice can show increases in BUN and creatinine levels at later ages, resulting in a similar pattern of renal insufficiency at that time. The combined assessment of BUN + creatinine + bicarbonate alone provided a unique prognostic marker set that unambiguously identified mice that were in the terminal stages of renal failure.

In addition to overt signs of renal failure, a subset of *mgb* mice had other findings similar to patients with obstructive uropathy. For instance, *mgb+/−* male mice had significantly higher serum potassium and chloride levels, consistent with the development of type IV hyperkalemic renal tubular acidosis. In addition, one *mgb+/−* female mouse also clearly developed polyuria and polydipsia. Finally, after percutaneous drainage, *mgb−/−* bladders rapidly refilled with 10 to 15 ml of urine, consistent with the development of polyuria. Taken together with the serum chemistry data, these findings suggest that *mgb* mice represent an excellent model for the study of obstructive uropathy.

The basis for the gender difference in viability between *mgb−/−* mice remains to be determined. Clearly, this difference in longevity could have a genetic basis involving either the *mgb* gene locus or other potential modifying loci. That female *mgb−/−* mice display a less severe bladder phenotype *in utero* may support this hypothesis. However, it also is plausible that the *mgb* phenotype is complicated by gender differences in anatomy. The urethra is significantly longer and more complex in the male mouse. This alone may hinder male *mgb−/−* mice from expressing sufficient quantities of urine after the development of megabladder, resulting in a faster disease progression. Morphologic evidence and serum chemistry data support this observation, because most female *mgb−/−* mice do not seem to develop as severe hydronephrosis or chronic renal failure as that observed in male mice.

To date, few genetic models of lower urinary tract obstruction have been described; however, congenital and postnatal hydronephrosis were reported previously in several mouse lines. A recessive mutation, known as congenital progressive hydronephrosis, that results in ureteropelvic obstruction has been reported in inbred *C57BL/6J* mice (28). ADAMTS-null mice also have been reported to develop hydronephrosis as a result of ureteropelvic blockage (29). Hydronephrosis also has been observed as a hereditary condition in male *C57BL/KsJ* mice, whereas mice that are deficient in the lysosomal membrane protein LIMP-2/LGP85 develop hydronephrosis that is

associated with a demyelinating peripheral neuropathy (30,31). Transgenic mice that overexpress human chorionic gonadotropin develop functional urethral obstruction that is associated with enlargement of prostates and seminal vesicles (32). None of the defects that are observed in these mice is similar to the *mgb−/−* phenotype, suggesting that the *mgb−/−* mouse is a unique transgenic model.

Conclusion

It is our working hypothesis that *mgb−/−* mice develop megabladder as a result of a tissue-specific defect in detrusor smooth muscle differentiation during embryonic development. The *mgb−/−* mouse therefore provides an exciting and unique resource for the examination of the basic cellular, molecular, and genetic mechanisms that are associated with bladder and lower urinary tract development and function *in vivo*. Although the *mgb−/−* mouse does not possess posterior urethral valves, the condition that is associated most commonly with lower urinary tract obstruction in children, the lack of smooth muscle development that is associated with the *mgb−/−* bladder produces the functional equivalent of an *in utero* lower urinary tract obstruction in mice. As a result, *mgb−/−* mice represent an excellent model of the subsequent pathologic events that are associated with posterior urethral valves, providing us with the first genetic model to study these events *in vivo*. It is important to note that the functional utility of the *mgb* mouse as a model of *in utero* lower urinary tract obstruction is independent of the identification of the gene loci that are responsible for the bladder defects that are observed in these mice. Continued studies of the *mgb−/−* mouse will enhance our understanding of urogenital development and pathogenesis, permitting the evaluation of pharmacologic, surgical, and gene therapy strategies to prevent and treat diseases that are associated with the bladder and the kidney.

Acknowledgments

These studies were supported partially by National Institutes of Health grant R01-DK70907 and R01-EY12995.

We thank the Comprehensive Cancer Center Mouse Phenotyping Shared Resource (The Ohio State University) and the Biomorphology Core at Columbus Children's Research Institute for assistance on this project.

Disclosures

None.

References

1. Jouannic JM, Hyett JA, Pandya P, Gulbis B, Rodeck C, Jauniaux E: Perinatal outcome in fetuses with megacystis in the first half of pregnancy. *Prenat Diagn* 23: 340–344, 2003
2. Pinette M, Blackstone J, Wax J, Cartin A: Enlarged fetal bladder: Differential diagnosis and outcomes. *J Clin Ultrasound* 31: 328–334, 2003
3. McHugo J, Whittle M: Enlarged fetal bladders: Aetiology, management and outcome. *Prenat Diagn* 21: 958–963, 2001
4. Executive Summary: United States Renal Data System Annual Data Report. *Am J Kidney Dis* 34[Suppl 1]: S9–S19, 1999
5. Foreman JW, Chan JM: Chronic renal failure in infants and children. *J Pediatr* 113: 793–800, 1988
6. Roth KS, Carter WH Jr, Chan JC: Obstructive nephropathy in children: Long-term progression after relief of posterior urethral valve. *Pediatrics* 107: 1004–1010, 2001
7. Zhao H, Yang Y, Rizo CM, Overbeek PA, Robinson ML: Insertion of a Pax6 consensus binding site into the alphaA-crystallin promoter acts as a lens epithelial cell enhancer in transgenic mice. *Invest Ophthalmol Vis Sci* 45: 1930–1939, 2004
8. Robinson ML, Overbeek PA, Verran DJ, Grizzle WE, Stockard CR, Friesel R, Maciag T, Thompson JA: Extracellular FGF-1 acts as a lens differentiation factor in transgenic mice. *Development* 121: 505–514, 1995
9. Taketo M, Hoopes C, Howard TA, Linney E, Seldin MF: Mapping of the mouse Rar loci encoding retinoic acid receptors RAR alpha, RAR beta and RAR gamma. *Jpn J Genet* 68: 175–184, 1993
10. Cammarata PR, Zhou C, Chen G, Singh I, Reeves RE, Kuszak JR, Robinson ML: A transgenic animal model of osmotic cataract. Part 1: Over-expression of bovine Na+/myo-inositol cotransporter in lens fibers. *Invest Ophthalmol Vis Sci* 40: 1727–1737, 1999
11. Goodrich LV, Johnson RL, Milenkovic L, McMahon JA, Scott MP: Conservation of the hedgehog/patched signaling pathway from flies to mice: Induction of a mouse patched gene by Hedgehog. *Genes Dev* 10: 301–312, 1996
12. Poladia DP, Kish K, Kutay B, Hains D, Kegg H, Zhao H, Bates CM: Role of fibroblast growth factor receptors 1 and 2 in the metanephric mesenchyme. *Dev Biol* 291: 325–339, 2006
13. Cunningham D, Xiao Q, Chatterjee A, Sulik K, Juriloff D, Elder F, Harrison W, Schuster G, Overbeek PA, Herman GE: Exma: An X-linked insertional mutation that disrupts forebrain and eye development. *Mamm Genome* 13: 179–185, 2002
14. McHugh KM: Molecular analysis of smooth muscle development in the mouse. *Dev Dyn* 204: 278–290, 1995
15. Bitgood M, McMahon A: Hedgehog and Bmp genes are coexpressed at many diverse sites of cell-cell interaction in the mouse embryo. *Dev Biol* 172: 126–138, 1995
16. Roberts D, Johnson R, Burke A, Nelson C, Morgan B, Tabin C: Sonic hedgehog is an endodermal signal inducing Bmp-4 and Hox genes during induction and regionalization of the chick hindgut. *Development* 121: 3163–3174, 1995
17. Apelqvist A, Ahlgren U, Edlund H: Sonic hedgehog directs specialized mesoderm differentiation in the intestine and pancreas. *Curr Biol* 7: 801–804, 1997
18. Marigo V, Davey R, Zuo Y, Cunningham J, Tabin C: Biochemical evidence that patched is the hedgehog receptor *Nature* 384: 176–179, 1996
19. Platt K, Michaud J, Joyner A: Expression of the mouse Gli and Ptc genes is adjacent to embryonic sources of hedgehog signals suggesting a conservation of pathways between flies and mice. *Mech Dev* 62: 121–135, 1997
20. Winnier G, Blessing M, Labosky P, Hogan B: Bone morphogenetic protein-4 is required for mesoderm formation and patterning in the mouse. *Genes Dev* 9: 2105–2116, 1995
21. Hogan B: Bone morphogenetic proteins: Multifunctional regulators of vertebrate development. *Genes Dev* 10: 1580–1594, 1996

22. Chen J, Kitchen C, Streb J, Miano J: Myocardin: A component of a molecular switch for smooth muscle differentiation. *J Mol Cell Cardiol* 34: 1345–1356, 2002
23. Majesky M: Decision, decisions. . .SRF coactivators and smooth muscle myogenesis. *Circ Res* 92: 824–826, 2003
24. Du K, Ip H, Li J, Chen M, Dandre F, Yu W, Lu M, Owens G, Parmacek M: Myocardin is a critical serum response factor cofactor in the transcriptional program regulating smooth muscle cell differentiation. *Mol Cell Biol* 23: 2425–2437, 2003
25. Wang Z, Wang D-Z, Hockemeyer D, McAnally J, Nordheim A, Olson E: Myocardin and ternary complex factors compete for SRF to control smooth muscle gene expression. *Nature* 428: 185–189, 2004
26. Brittingham J, Phiel C, Trzyna W, Gabbeta V, McHugh KM: Identification of distinct molecular phenotypes in cultured gastrointestinal smooth muscle cells. *Gastroenterology* 115: 605–617, 1998
27. McHugh KM: Molecular analysis of gastrointestinal smooth muscle development. *J Pediatr Gastroenterol Nutr* 32: 379–394, 1996
28. Horton CE Jr, Davidson MT, Jacobs JB, Berstein GT, Retik AB, Mandell J: Congenital progressive hydronephrosis in mice: A new recessive mutation. *J Urol* 140: 1310–1315, 1988
29. Weide LG, Lacy PE: Hereditary hydronephrosis in C57BL/KsJ mice. *Lab Anim Sci* 41: 415–418, 1991
30. Gamp AC, Tanaka Y, Lullmann-Raunch R, Wittke D, D'Hodge R, De Deyn PP, Moser T, Maier H, Hartmann D, Reiss K, Illert AL, von Figura K, Saftig P: LIMP-2/LGP85 deficiency causes ureteric pelvic junction obstruction, deafness and peripheral neuropathy in mice. *Hum Mol Genet* 15: 631–646, 2003
31. Yokoyama H, Wada T, Kobayashi K, Kuno K, Kurihara H, Shindo T, Matsushima K: A disintegrin and metalloproteinase obstructive nephropathy. *Nephrol Dial Transplant* 9: 39–41, 2002
32. Rulli SB, Ahriainen P: Makela S, Toppari J, Poutanen M, Huhtaniemi I: Elevated steroidogenesis, defective reproductive organs, and infertility in transgenic male mice overexpressing human chorionic gonadotropin. *Endocrinology* 144: 4980–4990, 2003

Supplemental information for this article is available online at http://www.jasn.org/.